Limnol. Oceanogr., 50(3), 2005, 850–863

Diel variations in the photosynthetic parameters of *Prochlorococcus* strain PCC 9511: Combined effects of light and cell cycle

F. Bruyant[1] *and M. Babin*

Laboratoire d'Océanographie de Villefranche, Université Pierre et Marie Curie and CNRS, BP 8, 06238 Villefranche sur Mer Cedex, France

B. Genty[2]

Laboratoire d'Ecophysiologie Végétale, Université Paris Sud and CNRS, 91405 Orsay, France

O. Prasil

Photosynthesis Research Center at the Institute of Microbiology AVCR and University of South Bohemia, Opatovicky mlyn, 37981 Trebon, Czech Republic

M. J. Behrenfeld[3]

NASA/GSFC, Code 970, Building 22, Greenbelt, Maryland 20771

H. Claustre and A. Bricaud

Laboratoire d'Océanographie de Villefranche, Université Pierre et Marie Curie and CNRS, BP 8, 06238 Villefranche sur Mer Cedex, France

L. Garczarek

Equipe Phytoplancton Océanique, Station Biologique, Université Pierre et Marie Curie and CNRS, BP 74, 29682 Roscoff Cedex, France

J. Holtzendorff[4]

Humboldt-University, Institute of Biology/Genetics, Chausseestrasse 117, D-10115 Berlin, Germany

M. Koblizek and *H. Dousova*

Photosynthesis Research Center at the Institute of Microbiology AVCR and University of South Bohemia, Opatovicky mlyn, 37981 Trebon, Czech Republic

F. Partensky

Equipe Phytoplancton Océanique, Station Biologique, Université Pierre et Marie Curie and CNRS, BP 74, 29682 Roscoff Cedex, France

---

[1] Present address: Dalhousie University, Department of Oceanography and IMB-NRC, Halifax, Nova Scotia B3H 4J1, Canada.

[2] Present address: CEA/Cadarache, DSV, DEVM, Laboratoire d'Ecophysiologie de la Photosynthèse, UMR 6191 CNRS-CEA-Aix Marseille 11, 13108 Sant-Paul-lez-Durance Cedex, France.

[3] Present address: Department of Botany and Plant Pathology, Cordley Hall 2082, Oregon State University, Corvalis, Oregon 97331.

[4] Present address: Equipe Phytoplancton Océanique, Station Biologique, Université Pierre et Marie Curie and CNRS, BP 74, 29682 Roscoff Cedex, France.

Acknowledgments

The results presented here were obtained during a workshop held in the framework of the European Commission research project PROMOLEC (contract MAS3-CT97-0128). We thank Ms. Florence Le Gall and Sandrine Boulben for preparing culture medium. M. Dominique Marie and Drs Daniel Vaulot, Stéphan Jacquet, and Jean Blanchot also greatly contributed to the success of this experiment by performing the flow-cytometric measurements and Ms Isabelle Mary, Dr Wolfgang Hess, and Jean-Claude Thomas by their participation in RNA sampling. We are grateful to Rosmarie Rippka for providing us with the axenic *Prochlorococcus* strain PCC9511 and to David d'Arena, who performed the HPLC analyses. O.P. and M.K. were supported by the projects Barrande 99026 and Ministry of Education LN00A141. M.J.B. was supported by the projects National Aeronautics and Space Administration UPN161-35-05-08 and RTOP622-52-58. We also thank Antoine Sciandra and Yannick Huot for helpful discussions and two anonymous referees for their constructive comments.

Abstract

We examined the mechanisms related to the diel variations in the parameters of the relationship between the rate of carbon fixation of phytoplankton and irradiance (*P* vs. *E* curve). Our goal was to understand what determines the phase of these variations relative to that of the light cycle. We grew the marine prokaryote *Prochlorococcus* in an axenic cyclostat culture system under a light–dark cycle that mimicked natural conditions at sea surface and followed changes in cell physiology with a 2-h resolution. Individual cells divide mostly in phase with each other, once a day at the beginning of the dark period. The quantum yields of chlorophyll fluorescence, the maximum quantum yield of carbon fixation (ϕ_{Cmax}) and the maximum rate of carbon fixation (P^B_{max}) exhibited diel variations over about factors of 2, 4, and 4, respectively, with maxima at the beginning of the light period. The morning drop in ϕ_{Cmax} and the quantum yield of fluorescence, which was accompanied by only a small decrease (<15%) of photochemial efficiency of PSII (F_v/F_m), suggests regulation by light and preceded the drop in P^B_{max} by 4 h. The decrease in P^B_{max} during the day matched a decrease in the transcription level of Rubisco. The quantum yield of fluorescence, ϕ_{Cmax}, and P^B_{max} increased again during the dark period, but this recovery was slowed at the time of cell division. Our results suggest that the pattern of diel variations in the photosynthetic parameters is determined both by photoacclimation and the cell-division cycle.

The photosynthetic parameters of phytoplankton derived from the relationship between the rate of carbon fixation and irradiance (so-called *P* vs. *E* curve) generally exhibit large diel variations in the marine environment (Harding et al. 1981*a*; Rivkin and Putt 1988). It has often been proposed that diel variations in the maximum chlorophyll-specific carbon fixation rate (P^B_{max}) and in the normalized initial slope of the *P* versus *E* curve (α^B) are controlled by an internal clock (Golden et al. 1997). It is unclear, however, what structural and functional changes of the photosynthetic apparatus are involved in P^B_{max} and α^B diel variations.

Highest values in P^B_{max} have most often been observed at midday (Prézelin and Matlick 1980) but have also been observed in the morning (Harding et al. 1981*a*) and even by night (Rivkin and Putt 1987). Diel variations in α^B most often parallel those of P^B_{max} (Rivkin and Putt 1988; Vandevelde et al. 1989). When P^B_{max} and α^B covary at the daily time scale and maximum values of α^B are observed by day (Babin et al. 1995), it is unlikely that photoacclimation is the driving process because then one would rather expect them to covary inversely (Dubinsky 1980). Harding et al. (1981*b*) noticed that the amplitude of variations in P^B_{max} covaried with changes in the growth rate of phytoplanktonic populations grown in batch cultures. This might indicate the influence of changes in the cell structure, related to the cell cycle. The results of Putt and Prézelin (1988), however, do not support a potential role of cell cycle.

Rivkin and Putt (1987) noticed that P^B_{max} peaks by day when midday irradiance is low to moderate and by night when midday irradiance is high. Interestingly, Vaulot and Marie (1999) observed strong diel variations in divinyl-chlorophyll *a* (div-Chl *a*) fluorescence of *Prochlorococcus* cells collected in the equatorial Pacific. A profound minimum was recorded around 1200 h for samples collected close to the sea surface, where high irradiance prevails, while the daily minimum was rather recorded by night for samples collected at depth. When the minima in P^B_{max} and α^B are observed by day, photoinhibition resulting from exposure of phytoplankton to high irradiance may be the cause and may mask the diel variations resulting from an endogenous rhythm. Photoinhibition is commonly observed at midday at the level of photosystem 2 activity, as revealed by nonphotochemical quenching of chlorophyll fluorescence (Kiefer 1973; Dandonneau and Neveux 1997). Behrenfeld et al. (1998) suggested that, at extreme irradiances such as those measurable close to the sea surface at low and medium latitudes, the rate-limiting step in carbon fixation may even become photosystem 2 activity.

As stated by Henley (1993), in his review on photoinhibition and diel changes of phytoplankton photosynthesis, the current challenge is to resolve the different processes that coincide in time and give rise to the bulk diel variations of the photosynthetic parameters. Our objective was to determine some of the functional changes that take place in the photosynthetic apparatus of phytoplankton over the course of the day.

This study was conducted on *Prochlorococcus*, which is the most abundant photosynthetic organism on Earth and is a major contributor to global primary production in oligotrophic areas of the world ocean (Partensky et al. 1999*a*). Natural variations of solar irradiance prevailing close to the sea surface were simulated with care. These light conditions were chosen to stimulate strong responses in the processes responsible for the diel variations in photosynthesis. We examined diel changes in photosynthetic properties both at the levels of carbon fixation and photosystem 2 activity. We also monitored changes in the gene transcription patterns of relevant components of photosystem 2 and dark reactions. Variations in the photosynthetic parameters of phytoplankton have been found to have a significant effect on primary production (Rivkin and Putt 1987). Using our observations on *Prochlorococcus*, we examined how the changes in photosynthetic parameters modulate primary production over the course of the day.

Materials and methods

Culturing system and sampling strategy—Two cyclostats of the oxyphotobacterium *Prochlorococcus* strain PCC 9511 (Rippka et al. 2000) were maintained in axenic conditions for more than 15 d (but see below). The entire culture device has been detailed elsewhere (Bruyant et al. 2001). Briefly, it was composed of two 20-liter polycarbonate flasks (Nalgene) containing 10 liters of the PCR S11 medium (Rippka

et al. 2000), continuously renewed with fresh medium at a mean rate of 8 ml min^{-1}. The culture flasks were placed between two sets of six dimmable neon tubes providing a smooth light–dark circadian cycle peaking at 970 μmol quanta m^{-2} s^{-1} that simulated light conditions in the ocean upper layer at low latitude. The temperature of the culture was maintained constant (21°C ±1°C) using thermostated water circulation. Biomass level was maintained by adjusting daily the medium renewal rate, based on flow cytometric cell counts performed at the dark-to-light transition. After 15 d of acclimation, the two cyclostats were extensively sampled during 4 full d. However, the data collected during the fourth day were discarded from the data set presented in the results section because, as indicated in Claustre et al. (2002), a slight bacterial contamination appeared and the cell density declined. Samples were collected every second hour in the first cyclostat (#1) for all analyses excluding gene transcription (see details below). In the second cyclostat (#2), samples were collected every fourth hour only for flow cytometry analyses, measurements of variable fluorescence, and gene transcription analyses. Flow-cytometry analyses and measurements of variable fluorescence allowed comparison between the two cyclostats.

Flow cytometry analyses—Cell numbers and DNA cell content were determined using a FacScan flow cytometer (Becton Dickinson). Immediately after sampling, cells were fixed with a mixture of 1% paraformaldehyde and 0.1% glutaraldehyde for 15 min (both chemicals from Sigma), then frozen in liquid nitrogen and stored at −80°C. Once thawed, cells were stained using a 1 : 10,000 dilution of the commercial solution of the DNA dye SYBR-Green I (Molecular Probes) and then analyzed according to Marie et al. (1999 and 2000). The same measurement allowed counting *Prochlorococcus* cell number and following diel variations in DNA cell content. It also allowed determining whether contaminant bacteria (particles without red fluorescence) were or were not present in the culture. Growth rates were derived from DNA synthesis data obtained from flow-cytometry measurements according to Carpenter and Chang (1988) (see details in Claustre et al. 2002).

Pigment analyses—The concentration of *Prochlorococcus* pigments was determined on the first cyclostat after filtration onto glass fiber filters (Whatman, GF/F) of 15 ml of culture (triplicates) (Claustre et al. 2002). The reverse-phase high-performance liquid chromatography (HPLC) protocol described by Vidussi et al. (1996) was applied with some modifications. Actually, in the present study, we used a flow rate of 0.5 ml min^{-1} and a reverse phase chromatographic column (RP-C8, Hypersil, MOS.3μm).

Light absorption coefficient—The optical density (OD) of *Prochlorococcus* was measured in triplicate between 190 and 800 nm with 1-nm increments on a sample of the culture suspension contained in a 1-cm quartz cuvette using a dual-beam spectrophotometer (Lambda 19, Perkin-Elmer) equipped with a 60-mm integrating sphere (Claustre et al. 2002). Filtered culture (onto 0.2-μm syringe filters) was used as reference. The *Prochlorococcus* absorption coefficient, [$a(\lambda)$ (m^{-1})] and chlorophyll-specific absorption coefficient [$a^*(\lambda)$ (m^2 mg div-Chl a^{-1})] were determined as in Claustre et al. (2002).

The absorption coefficient of photosynthetic pigments only [$a_{ps}(\lambda)$ (m^{-1})], i.e., for pigments contributing to light harvesting for photochemistry, was derived using the approach described in Babin et al. (1996) as

$$a_{ps}(\lambda) = a(\lambda)(1 - c_{nps}) \quad (1)$$

where c_{nps} (dimensionless) is the relative contribution of nonphotosynthetic pigments to light absorption. We assume that, in *Prochlorococcus*, the only nonphotosynthetic pigment is zeaxanthin (see Discussion). Divinyl-chlorophyll *a* and α-carotene were the only significant photosynthetic pigments.

The relative contribution of zeaxanthin to light absorption [$c_{nps}(\lambda)$; dimensionless] can be estimated as

$$c_{nps}(\lambda) = \frac{a^{sol}_{zea}(\lambda)\langle zea\rangle}{\sum_{all} a^{sol}_{m}(\lambda)\langle m\rangle} \quad (2)$$

where $a^{sol}_{zea}(\lambda)$ is the mass-specific absorption coefficient of zeaxanthin in solution (i.e., unpackaged) (m^2 mg^{-1}), $a^{sol}_{m}(\lambda)$ is the mass-specific absorption coefficient of the *m*th pigment in solution (m^2 mg^{-1}), $\langle zea\rangle$ is the concentration of zeaxanthin (mg m^{-3}), and $\langle m\rangle$ is the concentration of the *m*th pigment (mg m^{-3}). The numerator in Eq. 2 represents absorption by zeaxanthin and the denominator represents absorption by all pigments.

The $a^{sol}_{m}(\lambda)$ spectra for all significant *Prochlorococcus* pigments were determined on pigment extracts in solvent using a photodiode-array detector connected on the HPLC line (data not shown). The spectra were then wavelength shifted to obtain maximum absorption at the wavelengths (λ_{max}), where it is usually observed in vivo (Table 2). The spectra were also scaled using the $a^{sol}_{m}(\lambda_{max})$ given in Table 2.

Fluorescence measurements—In vivo div-Chl *a* fluorescence was measured by the pump and probe approach (Mauzerall 1972) using a Xe-PAM fluorometer (H. Walz GmbH). The nonactinic probe flashes were produced by a xenon lamp and filtered by a combination of a colored blue-green filter (BG39, 5 mm, Schott) and a short-pass filter (dichroic SP695, Walz). Saturating pump flashes were produced by a xenon flash lamp combined with a BG39 filter. Fluorescence emission was filtered by a combination of three long-pass filters (dichroic R65, Balzers; red RG645, 3 mm, Schott; red RG665, 1 mm, Schott). The fluorescence signal was monitored using a digital oscilloscope (Lecroy 9310C).

During the experiment, we measured the minimum and maximum fluorescence flash yields after a 30-min dark adaptation (F_o, F_m). F_o was measured by applying to the samples nonactinic probe flashes, while for F_m, the measuring probe flash was applied 50 μs after a saturating pump flash (Mauzerall 1972). We also measured the minimum and maximum fluorescence flash yields under light conditions prevailing in the cultures (F'_o and F'_m). These light conditions (as measured by an irradiance meter just before sampling) were reproduced inside the cell holder of the PAM using actinic light generated by a halogen lamp equipped with a short-pass filter (dichroic SP695, Walz). The measurement

Table 1. Symbols and abbreviations.

Symbol or abbreviation	Full name	Units
PSI	Photosystem 1	
PSII	Photosystem 2	
Q_A	Plastoquinone Q_A	
Q_B	Plastoquinone Q_B	
FRR	Fast repetition rate	
PAM	Pulse amplitude modulated	
DCMU	3-(3,4-dichloro-phenyl)-1,1-dimethylurea	
DMSO	Di-methyl sulfoxide	
F_x	Fluorescence flash level of in vivo chlorophyll *a* fluorescence determined after dark adaptation. Subscript *x* may be *o* for minimum, *m* for maximum, *v* for variable.	Relative units
F'_x	Fluorescence flash level of in vivo chlorophyll *a* fluorescence determined immediately after sampling. Subscript *x* may be *o* for minimum or *m* for maximum.	Relative units
ϕ_{F_x}	Quantum yield of in vivo chlorophyll *a* fluorescence determined after dark adaptation. Subscript *x* may be *o* for minimum, *m* for maximum, *v* for variable.	Relative units
$\phi^{ps}_{F_x}$	Quantum yields of in vivo chlorophyll *a* fluorescence calculated for photosynthetic pigments only	Relative units
ϕ'_{F_x}	Quantum yield of in vivo chlorophyll *a* fluorescence determined immediately after sampling. Subscript *x* may be *o* for minimum or *m* for maximum.	Relative unit
F_v/F_m	Photochemical efficiency of PSII	Dimensionless
σ_{PS2}	Effective absorption cross-section of PSII	m^2 (mol photon)$^{-1}$
$t_{½}$	Half-life time of recovery in the quantum yields of in vivo chlorophyll *a* fluorescence from quenching, in the dark	Hours
K_q	Rate constant for quenching of fluorescence under continuous light	h^{-1}
K_r	Rate constant for recovery of fluorescence from quenching under continuous light or in the dark	h^{-1}
τ	Turnover time for PS2 photochemistry under continuous light	h
PAR	Photosynthetic available radiation	μmol quanta m^{-2} s^{-1}
div-Chl *a*	Divinyl-chlorophyll *a*	
OD (λ)	Optical density	Dimensionless
a (λ)	Absorption coefficient	m^{-1}
$a^*(\lambda)$	Chlorophyll-specific absorption coefficient	m^2 (mg div-chl *a*)$^{-1}$
$\bar{a}^*$	Mean chlorophyll-specific absorption coefficient	m^2 (mg div-chl *a*)$^{-1}$
$a^{ps}(\lambda)$	Absorption coefficient of photosynthetic pigments only	m^{-1}
$a^{sol}_{zea}(\lambda)$	Mass-specific absorption coefficient of zeaxanthin in solution (i.e., unpackaged)	m^2 mg^{-1}
$a^{sol}_m(\lambda)$	Mass-specific absorption coefficient of the *m*th pigment in solution	m^2 mg^{-1}
c_{nps}	Relative contribution of nonphotosynthetic pigments to light absorption	Dimensionless
DIC	Dissolved inorganic carbon	
α^B	Chlorophyll specific photosynthetic efficiency	mg C (mg div-chl *a*)$^{-1}$ h^{-1} (μmol quanta m^{-2} s^{-1})$^{-1}$
P^B	Chlorophyll specific carbon fixation rate	mg C (mg div-chl *a*)$^{-1}$ h^{-1}
P^B_{max}	Maximum chlorophyll specific carbon fixation rate	mg C (mg div-chl *a*)$^{-1}$ h^{-1}
ϕ_{Cmax}	Maximum quantum yield of carbon fixation	mol C (mol quanta)$^{-1}$
$\phi^{PS}_{C\ max}$	Maximum quantum yield of carbon fixation calculated for photosynthetic pigments only	mol C (mol quanta)$^{-1}$
E_K	Saturation parameter	μmol quanta m^{-2} s^{-1}
Θ^B	Cumulated amount of carbon fixed	mg C (mg div-chl *a*)$^{-1}$
Rubisco	Ribulose 1-5 bi-phosphate carboxylase oxygenase	
rbcL	Gene encoding the large sub-unit of the Rubisco protein	
pcbA	Gene encoding the major light harvesting complex of PSII	
psbA	Gene encoding the D1 protein of reaction center 2	

Table 2. Wavelength of maximum in vivo absorption (λ_{max}), and pigment mass-specific absorption coefficient at $\lambda_{max}[a^*_m(\lambda_{max})]$ for all pigments that contributed significantly to light absorption by *Prochlorococcus* during this experiment. For divinyl-chlorophyll *a*, λ_{max} was obtained from in vivo absorption spectra. For zeaxanthin and α-carotene, λ_{max} was derived from our measurements of $a^{sol}_m(\lambda)$, wavelength shifted according to Bidigare et al. (1990). Only shifts given for the blue part of the spectrum were considered as, over 550 nm, zeaxanthin has no significant contribution in *Prochlorococcus* absorption. Note that divinyl-chlorophyll *b* was undetectable during this experiment (Claustre et al. 2002). The $a^{sol}_m(\lambda_{max})$ values used to scale the $a^{sol}_m(\lambda)$ spectra were taken from Goericke and Repeta (1993) for divinyl-chlorophyll *a* and zeaxanthin and from Bidigare et al. (1990) for α-carotene.

Pigment	λ_{max} (nm)	$a^{sol}_m(\lambda_{max})$ (m^2 mg^{-1})
Divinyl-chlorophyll *a*	445	0.0266
Zeaxanthin	462	0.0538
α-Carotene	457	0.0603

of F'_m was measured similarly to F_m, but under actinic light. F'_o was measured immediately after turning off the actinic light. For the different sets of F_o and F_m measurements, we calculated the photochemical efficiency of photosystem 2, F_v/F_m, with F_v being variable fluorescence (as calculated from $F_m - F_o$).

The recovery of fluorescence from quenching in the dark was monitored at time of maximum photosynthetic available radiation (PAR). Immediately after sampling and 30-min dark adaptation, a culture aliquot was kept in the dark and F_o and F_m were repeatedly measured at 5-min intervals until an asymptotic value was reached. This allowed us to determine the half-life time ($t_{1/2}$) and rate constant (K_r) of recovery from quenching for both F_o and F_m by fitting a first-order kinetic function to the data. The value obtained for K_r was the same for both F_o and F_m (see Results section).

The fast repetition rate fluorometer (FRR) described by Kolber et al. (1998) was used during the main experiment to measure F_o and F_m and the functional cross-section of photosystem 2 (σ_{PS2}) as described in Steglich et al. (2001).

The quantum yields for minimum and maximum fluorescence were calculated as

$$\phi_{F_x} = \frac{F_x}{\int_{400}^{700} a(\lambda)E_{probe}(\lambda)\, d\lambda} \quad (3)$$

where subscript *x* is *o* or *m* and $E_{probe}(\lambda)$ is irradiance of the Xe-PAM probe flash measured in relative units using a spectroradiometer (LI-COR, LI-1800UW) equipped with a cosine collector (0.7-mm diameter) fixed at the end of a 2-m optic fiber. The quantum yields of fluorescence were also calculated for photosynthetic pigments only ($\phi^{ps}_{F_x}$) by replacing $a(\lambda)$ by $a^{ps}(\lambda)$ in Eq. 3.

For assessing the occurrence of energy-dependent (transthylakoid ΔpH) quenching of fluorescence, 2 mmol L^{-1} ammonium chloride and 5 μmol L^{-1} gramicidin were used as uncouplers, and 0.5 μmol L^{-1} 3-(3,4-dichloro-phenyl)-1,1-dimethylurea (DCMU) as inhibitor of Q_A–Q_B electron transfer at PSII (final concentrations in the culture sample). Stock solution of gramicidin and DCMU were prepared in ethanol and dimethyl sulfoxide (DMSO), respectively.

Parameters of the carbon fixation versus light relationship—The relationship between the rate of carbon fixation and irradiance was determined in duplicate every second hour according to Lewis and Smith (1983). A 50-ml culture sample was collected in cyclostat 1, subdivided into two subsamples (replicates), and inoculated with inorganic ^{14}C ($NaH^{14}CO_3$, 2 μCi ml^{-1}). To determine the total activity of bicarbonate added, three 50-μl aliquots were added to 50 μl of an organic base (ethanolamin), 1 ml of distilled water, and 10 ml of the scintillation cocktail (90% Aquasol-2 Packard + 10% methanol) into glass scintillation vials. Then 1-ml aliquots of the inoculated subsample were dispensed into twenty 20-ml glass scintillation vials and placed within separate thermoregulated alveoli (21°C $\pm$1°C) at 20 different light levels. Light in the incubator was provided from the bottom by a metal halide lamp (OSRAM, Powerstar HQI-TS 150 W/NDL UVS) filtered through a water screen, a plexiglas white-diffusing plate, and different combinations of neutral gelatin filters (Kodak). The PAR (μmol quanta m^{-2} s^{-1}) in each alveolus was measured twice a day with an irradiance meter (Biospherical QSL-100) equipped with a 4π spherical quantum sensor. After 20 min of incubation, culture aliquots were acidified (1 ml of 1 mol L^{-1} HCl) and placed under the fuming hood for 1 h. Then 10 ml of the scintillation cocktail were added to each vial. The total concentration of dissolved inorganic carbon (DIC) was monitored during one of the replicate experiments. It was measured every second hour using a total organic carbon analyzer (Shimadzu TOC-5000) on a 10-ml aliquot to which 10 μl of 1 mol L^{-1} $HgCl_2$ were added. It was found to vary by less than $\pm$30% around 11 g m^{-3}. The chlorophyll-specific carbon fixation rate [P^B; mg C (mg div-Chl *a*)$^{-1}$ h^{-1}] was finally computed according to Parsons et al. (1984) using the latter mean value as DIC concentration. The initial slope of the *P* versus *E* curve [α^B mg C (mg div-Chl *a*)$^{-1}$ h^{-1} (μmol quanta m^{-2} s^{-1})$^{-1}$] and the maximum chlorophyll-specific carbon fixation rate [P^B_{max} mg C (mg div-Chl *a*)$^{-1}$ h^{-1}] were estimated by fitting the following equation (Jassby and Platt 1976) to the experimental P^B and PAR values (r^2 between 0.97 and 1.00):

$$P^B = P^B_{max}\tanh\left(\frac{\alpha^B \mathrm{PAR}}{P^B_{max}}\right) + P^B_0 \quad (4)$$

where P^B_0 is the estimated intercept. The light saturation parameter, E_K (μmol quanta m^{-2} s^{-1}), is defined as

$$E_K = \frac{P^B_{max}}{\alpha^B} \quad (5)$$

The maximum quantum yield of carbon fixation [ϕ_{Cmax}; mol C (mol quanta) $^{-1}$] was derived from

$$\phi_{Cmax} = \frac{\alpha^B}{\bar{a}^*} \quad (6)$$

where $\bar{a}^*$ is the mean chlorophyll-specific absorption coef-

ficient weighted by the spectral output of the incubation light source [$E(\lambda)$; μmol quanta m^{-2} s^{-1}],

$$\bar{a}^* = \frac{\int_{400}^{700} a^*(\lambda)E(\lambda)\, d\lambda}{\int_{400}^{700} E(\lambda)\, d\lambda} \quad (7)$$

The maximum quantum yield of carbon fixation for photosynthetic pigments only (ϕ^{PS}_{Cmax}) was calculated by replacing $a^*(\lambda)$ by $a^*_{PS}(\lambda)$ in Eq. 7.

RNA extraction, Northern blotting, and real-time RT-PCR—Total RNA was extracted as previously described (Hess et al. 1995) from a 400-ml culture collected from cyclostat #2 every 4 h. Transcription patterns for the *psbA* (coding for the *D1* protein of the reaction center 2) and *pcbA* (coding for the major light harvesting complex of PS2) genes, were obtained by northern blotting as described by Garczarek et al. (2000).

Transcription pattern for the *rbcL* gene (coding the large subunit of Rubisco protein) was obtained by quantitative real-time polymerase chain reaction (RT-PCR) using the *rnpB* gene (encoding RNase P RNA) (Hess et al. 1998) as an internal control to normalize for total RNA. Gene-specific RT-PCR primers for *rbcL,* rbcLMED 4-55F (CCTGAATATGTCCCCCTCGA) and rbcLMED 4-145R (CCGCTGCTGCAACTTCTTCT) and for *rnpB,* rnpBPCC 9511-1F (TTGAGGAAAGTCCGGGCTC) and rnpBPCC 9511-91R (GCGGTATGTTTCTGTGGCACT) were designed from the total genome sequence of *Prochlorococcus* MED 4 (http://genome.jgi-psf.org/microbial/) using PrimerExpress software from Applied Biosystems. Reverse transcription was carried out with the gene-specific reverse primers using SuperScriptII (Gibco-BRL) reverse transcriptase on 100 ng of DNAseI (Ambion) digested RNA.

RT-PCR was performed using the GeneAmp 5700 sequence detection system and SYBR Green PCR core reagents, both from Perkin Elmer, yielding a 122-base pair (bp) amplification product for the *rnpB* gene and a 79-bp product for the *rbcL* gene. PCR and data analysis were performed as described in Holtzendorff et al. (2002).

Statistical analyses—To verify (1) the possible occurrence of a drift over time in the diel variation pattern of individual variables (e.g., time of a maximum recorded later from day to day) and (2) the timing between the variation transients of two variables, we applied lag-time correlation analyses (Priestley 1994). In the first case, this analysis consists of performing a correlation analysis between the data of a given variable, collected during different sampling days. The data collected at the same time (lag = 0 h) or at times separated by a given lag (multiple of the sampling period, lag = 2, 4, . . . h) are paired. The absence of a day-to-day drift in variation patterns is confirmed when the best correlation coefficient is obtained with the same lag from day to day. In the second case, the correlation analysis is performed between the data of two different variables for the whole data set or for specified temporal windows (e.g., all data collected between 0600 and 1200 h). As in the first case, the data collected at the same time or at times separated by a given lag are paired. The temporal coincidence between transients of two variables is confirmed when the best correlation coefficient is obtained with no lag.

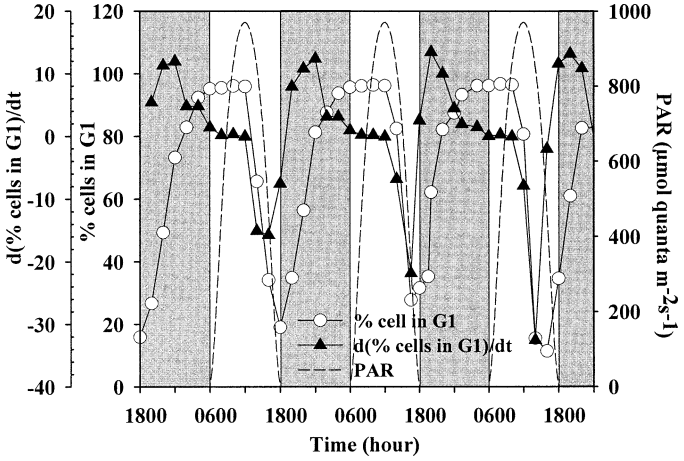

Fig. 1. Diel changes in the PAR (μmol quanta m^{-2} s^{-1}), in the percentage of cells in G1 phase and in the first derivative of this percentage indicating the intensity of the cell division process.

Results

Synchronization of Prochlorococcus *growth, and cell cycle*—Figure 1 shows the variations of the percentage of cells in G1 phase (%G1), i.e., cells that are not synthesizing DNA nor dividing, and of the first derivative of this value (d(%G1)/dt). The initial decrease of %G1 depicts the start time of DNA replication whereas the reincrease of %G1 corresponds to the release of daughter cells after division. The limits of the active cell-division period can better be visualized as the period when d(%G1)/dt is increasing (i.e., 1600–0000 h), the maximum rate being reached between 2000 and 0000 h. Thus, cell division mainly occurred during the first half of the night. The diel changes in the percentage of cells in S and G2 phase (data shown in Claustre et al. 2002) were also very reproducible over the 3 d of sampling. Consequently, the growth rates calculated from DNA synthesis rhythms (Carpenter and Chang 1988) were highly reproducible as well; $\mu = 0.69 \pm 0.04$ d^{-1} (see Claustre et al. 2002 for details).

Pigment concentrations—The amount of zeaxanthin/cell showed strong diel changes (nearly a factor of two), increasing during the day and decreasing during the night. The cellular content of div-Chl *a* showed smaller diel changes (over a factor of 1.5), decreasing during the day and rising up quickly just before the beginning of the light period. Detailed results on pigment content were presented by Claustre et al. (2002).

Photosystem 2 functional properties—Both ϕ_{F_o} and ϕ_{F_m} (as measured using the Xe-PAM fluorometer) showed strong diel variations with a diurnal decrease by ~50% (Fig. 2A).

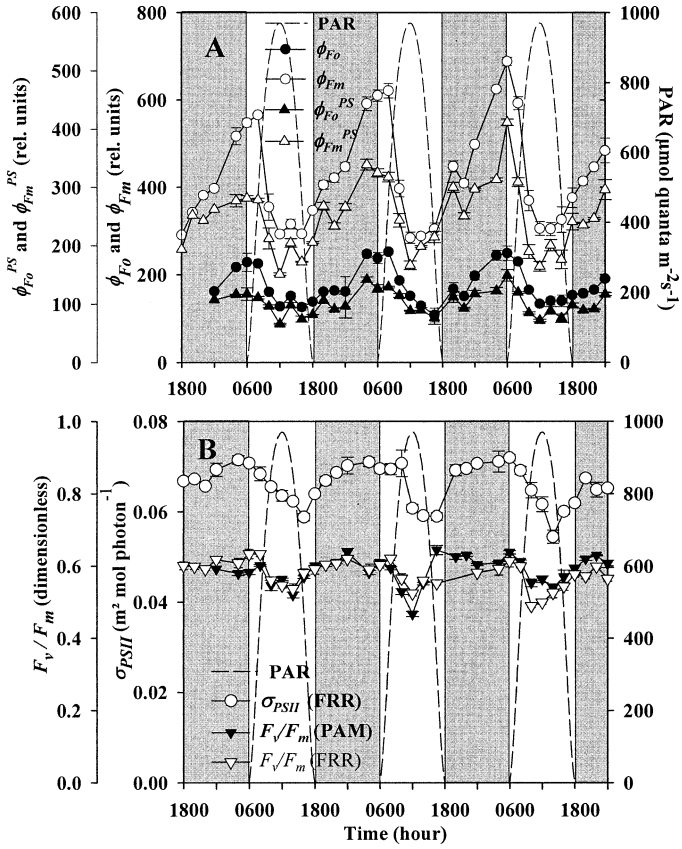

Fig. 2. (A) Diel changes in the PAR (μmol quanta m^{-2} s^{-1}), in the minimum (ϕ_{F_0}, $\phi_{F_0}^{PS}$, relative units) and the maximum (ϕ_{F_m}, $\phi_{F_m}^{PS}$, relative units) quantum yields of in vivo fluorescence measured after 30 min of dark adaptation using the Xe-PAM fluorometer (PS superscripts indicate quantum yields calculated for photosynthetic pigments only). Error bars indicates ± standard deviation. (B) Diel changes in the PAR (μmol quanta m^{-2} s^{-1}) in the photochemical efficiency of photosystem 2 (F_v/F_m, dimensionless) acquired using the FRR fluorometry and pump and probe technique and in the effective absorption cross-section of PSII (σ_{PS2}, m^2 (mol photon)$^{-1}$) determined using the FRR technique. Error bars indicate ± standard deviation.

The similar trends in ϕ_{F_o} and ϕ_{F_m} were characterized by a sharp decrease at the beginning of the light period (0600–1000 h), with minimum values reached around noon, and then an increase that lasted until the end of the dark period (0600 h the next day), with a transient slowing down of the increase between 2100 h and 0000 h. The highest quantum yields were measured at or 2 h after light onset. The quantum yields of fluorescence determined for photosynthetic pigments only showed very similar trends (Fig. 2A), with, however, a diurnal decrease of about 45%. The possible occurrence of day-to-day drifts in ϕ_{F_o} and ϕ_{F_m} variation patterns has been checked using a lag-time correlation analysis. For all days, both parameters are best inversely correlated with PAR between 0600 h and noon when a lag time of 2 h is applied (ϕ_{F_o} and ϕ_{F_m} starting to decrease 2 h after PAR starts to increase), indicating the absence of temporal drift in the data (day 1 $r^2 = 0.96$, $n = 4$; day 2 $r^2 = 0.98$, $n = 4$; day 3 $r^2 = 0.98$, $n = 4$, all with lag time = 2 h). The range and pattern of ϕ'_{F_o} and ϕ'_{F_m} variations were very similar to those of ϕ_{F_o} and ϕ_{F_m} (i.e., a diurnal decrease by ~50%; data not shown). The rate constant for recovery of ϕ_{F_o} and ϕ_{F_m} from quenching (K_r) was, on average, 0.283 ±0.052 h^{-1} ($t_{1/2}$ ~ 2.45 h).

The magnitude and trend in F_v/F_m variations (as determined using both the pump and probe and FRR fluorometry) were similar with the two protocols during the first 2 d, but slight discrepancies occurred afterward (Fig. 2B). Both F_v/F_m and σ_{PS2} (the latter determined by FRR fluorometry only) decreased by about 15% and 20%, respectively, as PAR increased (Fig. 2B). The minimal values for F_v/F_m were observed at a variable time around noon, while they were systematically observed at the end of the day (between 1600 and 1800 h) for σ_{PS2}. Both parameters are best inversely correlated with PAR between 0600 and 1800 h with a lag time of 0 (F_v/F_m, day 1 $r^2 = 0.432$, $n = 11$; day 2 $r^2 = 0.70$, $n = 10$; day 3 $r^2 = 0.75$, $n = 11$) or 2 h (σ_{PS2} starting to decrease 2 h after PAR starts to increase, day 1 $r^2 = 0.74$, $n = 12$; day 2 $r^2 = 0.98$, $n = 8$; day 3 $r^2 = 0.79$, $n = 10$), indicating the absence of drift in the data. Both F_v/F_m and σ_{PS2} increased to their maximum at or shortly after dusk. The highest F_v/F_m values were around 0.63, a typical value for nutrient-replete cultures in balanced growth (Parkhill et al. 2001).

Photosynthetic parameters—$\bar{a}^*$ showed diel changes (Fig. 3A), with values increasing by about 30% during the day and decreasing during the night, due to the diel changes in the zeaxanthin/div-Chl *a* ratio (Claustre et al. 2002). ϕ_{Cmax} and ϕ_{Cmax}^{ps} peaked at 0600 h (or 2 h before) and exhibited a sharp decrease by ~70% and 75%, respectively, as PAR increased (between 0600 h and noon) (Fig. 3B). Then ϕ_{Cmax} and ϕ_{Cmax}^{ps} remained low from around noon to around 0000 h and returned to their highest value just before the dark-to-light transition (Fig. 3B). We applied lag-time correlation analyses between ϕ_{Cmax} values and PAR (Priestley 1994). The inverse correlation is maximum between 0600 h and noon for a lag time of 4 h ($r^2 = 0.84$, $n = 12$, relation significant to the 1% level). The ϕ_{Cmax} and ϕ_{Cmax}^{ps} peak values were about half and close to the theoretical maximum of 0.125 mol C (mol quanta)$^{-1}$, respectively. Given the moderate changes in $\bar{a}^*$, the diel variations in α^B were very similar to those of ϕ_{Cmax} (Fig. 4A). It decreased by ~60% between 0600 h and noon, and remained low between 1200 and 000 h. The maximum α^B values were reached just before the beginning of the next light period (at 0600 h the next day) (Fig. 4A).

P_{max}^B also showed strong diel variations (Fig. 4B). After a peak at ~1000 h, i.e., about 4 h after that of ϕ_{Cmax}, P_{max}^B first exhibited a dramatic drop and then a slower decrease between 1200 and 0000 h. It showed an overall diurnal decrease of ~70%. It increased sharply between 0000 h and around 1000 h. A break in this increase was systematically observed at light onset. This variation pattern for P_{max}^B was particularly clear during the second and third sampling days. When performing a lag-correlation analysis between P_{max}^B and PAR on the data collected between 1000 and 0000 h, the inverse correlation is always maximum for a lag time of 4 h (P_{max}^B starting to decrease 4 h after PAR starts to increase)

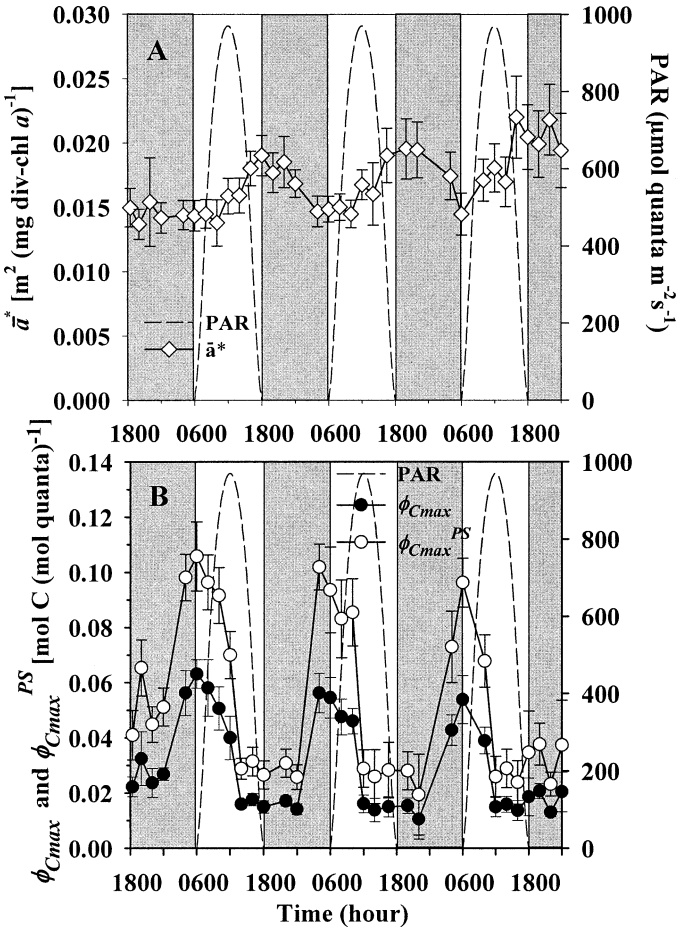

Fig. 3. (A) Diel changes in the PAR (μmol quanta m^{-2} s^{-1}) and in the mean chlorophyll specific absorption coefficient ($\bar{a}^*$, m^2 (mg div-Chl a)$^{-1}$) obtained for *Prochlorococcus* over 3 consecutive d of sampling. Error bars indicates ± standard deviation. (B) Diel changes in the PAR (μmol quanta m^{-2} s^{-1}), in the maximum quantum yield of carbon fixation (ϕ_{Cmax}, mol C [mol quanta]$^{-1}$) and in the maximum quantum yield of carbon fixation for photosynthetic pigments only (ϕ_{Cmax}, mol C [mol quanta]$^{-1}$). Error bars indicate ± standard deviation.

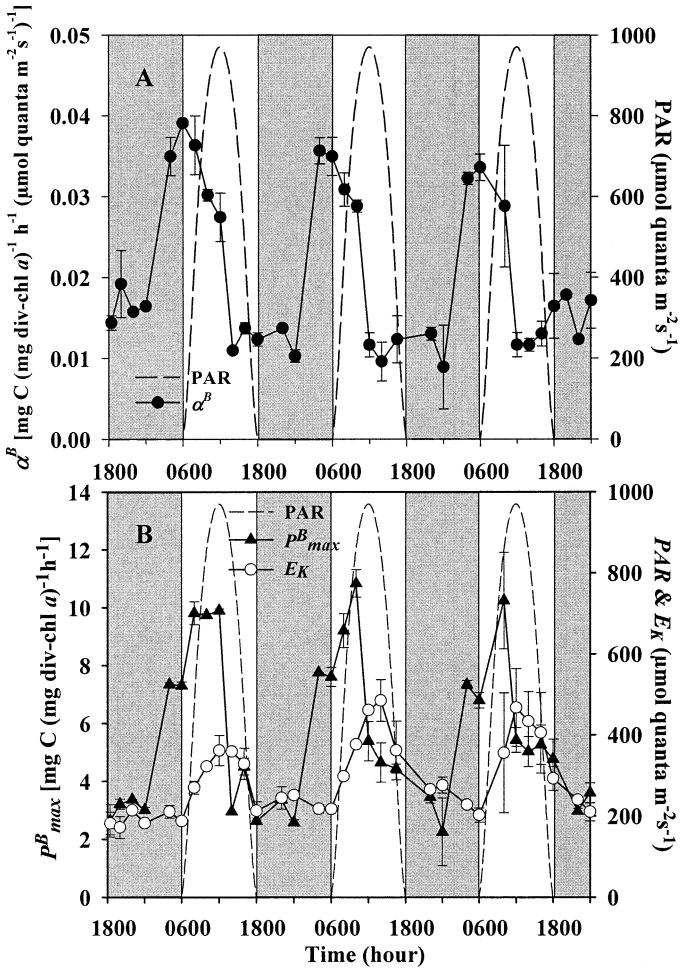

Fig. 4. (A) Diel changes in the PAR (μmol quanta m^{-2} s^{-1}) and in the chlorophyll-specific photosynthetic efficiency α^B (mg C (mg div-Chl a)$^{-1}$ h^{-1} (μmol quanta m^{-2} s^{-1})$^{-1}$) obtained over the 3 consecutive d of sampling. Error bars indicates ± standard deviation. (B) Diel changes in the PAR (μmol quanta m^{-2} s^{-1}), in the maximum chlorophyll-specific carbon fixation rate (P^B_{max}, mg C (mg div-Chl a)$^{-1}$ h^{-1}) and in the saturation parameter (E_K, μmol quanta m^{-2} s^{-1}) obtained over the 3 consecutive d of sampling. Error bars indicate ± standard deviation.

both if we consider each day separately or the sampling period as a whole (day 1 $r^2 = 0.84$, $n = 4$; day 2 $r^2 = 0.94$, $n = 3$; day 3 $r^2 = 0.80$, $n = 4$). This consistency confirms the absence of any drift in our observations and, therefore, that our culture was growing at steady state. During the 3 d of sampling, P^B_{max} reached relatively high values, around 10 mg C (mg div-Chl a)$^{-1}$ h^{-1}. The diel cycle in E_K, with a decrease by night of about 50%, was nearly in phase relative to the PAR cycle (Fig. 4B). Indeed, when performing a lag-correlation analysis between E_K and PAR over the 0600–1800 h time window, the correlation is maximum for a lag time of 0 h, both if we consider each day separately or the sampling period as a whole (P^B_{max} $r^2 = 0.6847$, $n = 19$, relation significant to the 1% level). E_k changed in such a way (values lower than PAR values) that the carbon fixation remained at saturation (close to P^B_{max}) for most of the light period (see below). Note that average E_K over one diel cycle is close to average PAR (~300 μmol quanta m^{-2} s^{-1}).

Diel changes in the photosynthetic parameters on a per cell basis (P^{cell}_{max}, the maximum rate of carbon fixation per cell, and α^{cell}, the photosynthetic efficiency per cell) have been examined (data not shown). The diel patterns were reproducible along the 3 d of sampling and very similar to those of the photosynthetic parameters normalized on a chlorophyll basis.

Transcription level of rbcL, psbA, and pcbA genes—The transcription level of the *rbcL* gene encoding the large subunit of the Rubisco protein was evaluated through the quantity of mRNA found in the cells. It provides an index of the level of transcripts but not necessarily of protein concentration in the cell. Transcript accumulation increased from the beginning of the dark period (1800 h) to a maximum at 0800 h (Fig. 5). Afterward, the amount of *rbcL* transcript decreased sharply down to nearly zero at the end of the light

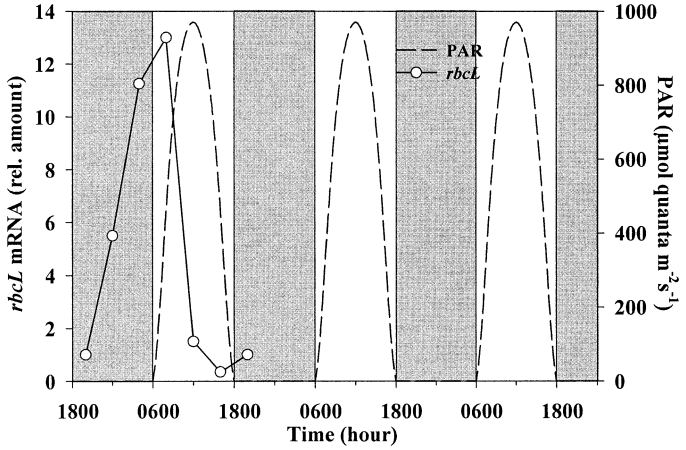

Fig. 5. Relative level of *rbcL* mRNA (encoding the large subunit of the Rubisco protein) shown alongside changes in PAR (μmol quanta m^{-2} s^{-1}). The relative level of transcription was normalized by the expression of the *rnpB* gene.

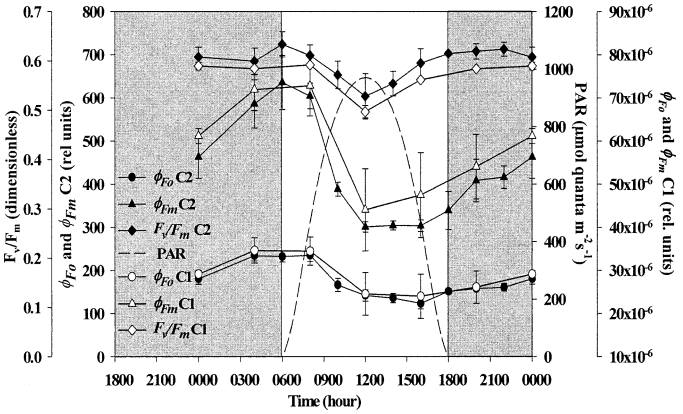

Fig. 6. Diel changes in the PAR (μmol quanta m^{-2} s^{-1}), minimum (ϕ_{F_o}) and maximum (ϕ_{F_m}) quantum yield of in vivo chlorophyll *a* fluorescence (relative units) and in the photochemical efficiency of photosystem 2 (F_v/F_m, dimensionless); measured on both cyclostat 1 and 2. Data are averaged over the 3 d of sampling and presented with standard deviations.

period. The transcription level of both *psbA* and *pcbA* genes showed strong diel changes, as has been described in detail in Garczarek et al. (2001). Briefly, the *psbA* transcription pattern followed closely the course of the light cycle, while the transcription of *pcbA* gene showed a bimodal pattern with one minimum of transcription at the beginning of the light period and another minimum at the beginning of the night. It is worth noting that *psbA* and *pcbA* are transcriptionally regulated, the light intensity being the triggering signal (Schaefer and Golden 1989; Axmann et al. 2003 for *rbcL*).

Discussion

The use of a cyclostat with modulated light allowed strong synchronization of both the cell cycle (Fig. 1, see also Holtzendorff et al. 2001) and the photosynthetic properties of *Prochlorococcus* PCC 9511 cultures and maintaining the phytoplanktonic population in exponential phase at a high growth rate (~0.69 d^{-1}, i.e., one division per day) during the whole sampling period (Claustre et al. 2002). Such a good synchrony was critical to better understanding the temporal succession of the different events of photosynthesis (light and dark reactions) as well as the interrelationship between the cell cycle and the different photosynthetic parameters that were measured. The light conditions we applied represent very well those encountered by *Prochlorococcus* in its natural environment close to the ocean surface. The high biomasses (around 150×10^6 cell ml^{-1}) reached in our cultures are, on the other hand, not representative of the oligotrophic systems where *Prochlorococcus* is always observed. Nevertheless, some of our results are comparable with observations made on natural populations of *Prochlorococcus.* This is the case, for instance, for the maximum carbon fixation rate per unit cell (P_{max}^{cell}). It was found to be between 0.6 and 4 fg C $cell^{-1}$ h^{-1} in the Moroccan upwelling, while it was between 0.8 and 4.8 fg C $cell^{-1}$ h^{-1} in our study (Partensky et al. 1999*b*).

To verify the reproducibility of our experiment, variable fluorescence (Fig. 6) and flow-cytometry parameters were measured on both cyclostat 1 and 2. We observed good agreement between the two cyclostats. In Fig. 6, the three 24-h cycles are averaged; standard deviation is shown for each sampling time. The low standard deviations observed in general also indicate good reproducibility of the variation patterns.

Photosystem 2 function—Striking diel variations were observed in ϕ_{F_o} and ϕ_{F_m} (a factor of two). Diel variations of even larger amplitude have been reported for *Prochlorococcus* collected in the equatorial Pacific at the level of fluorescence per cell, with a strong decrease during the day (Vaulot and Marie 1999). The magnitude and patterns of the variations we observed were the same whether measurements were made after 30 min of dark adaptation (ϕ_{F_o} and ϕ_{F_m}; Fig. 2A) or made at steady state under growth illumination (ϕ'_{F_o} and ϕ'_{F_m}; data not shown), which suggests that no short-lifetime nonphotochemical quenching of fluorescence occurred (see Falkowski and Raven 1997 for a review on nonphotochemical quenching in phytoplankton). The absence of effect of ammonium chloride and gramicidin on the recovery kinetic of nonphotochemical fluorescence quenching (data not shown) specifically indicates that no significant energy-dependent fluorescence quenching controlled by ΔpH (the major source of short-lifetime nonphotochemical quenching) took place, as often reported for cyanobacteria (reviewed by Campbell et al. 1998).

The large and parallel decrease in ϕ_{F_o} and ϕ_{F_m} (~50%) was accompanied by only a small decrease in F_v/F_m. The parallel decrease in ϕ_{F_o} and ϕ_{F_m} can be partly explained by changes in the effective absorption cross-section of PSII as σ_{PS2} decreased by ~20% during the light period (Fig. 2B). The decrease in σ_{PS2}, which cannot be attributed to energy-dependent quenching (see previous paragraph), may reflect state transition, a common phenomenon in cyanobacteria (Falkowski and Raven 1997; Campbell et al. 1998). This acclimation process has not yet been demonstrated in *Proch-*

lorococcus spp. and more generally is still a subject of debate in Chl *b*-containing oxyphotobacteria (Partensky and Garczarek 2003).

The rate constant for recovery of ϕ_{F_o} and ϕ_{F_m} from quenching in the dark ($K_r = 0.283 \pm 0.052$ h^{-1}, $t_{1/2} \sim 2.45$ h) is also incompatible with the commonly reported kinetic of state transitions for which $t_{1/2}$ is typically at minute scale in cyanobacteria (Campbell et al. 1998). In any case, the changes we observed in σ_{PS2} can only explain a part of the variations observed in ϕ_{F_o} and ϕ_{F_m}. Large nonphotochemical quenching induced by photoinhibition is also unlikely because it is generally not accompanied by a decrease of ϕ_{F_o} (see the review by Krause and Weis 1991). Thus, even if state transition and/or other processes (e.g., spillover from PSII to PSI) occurred, additional unidentified nonphotochemical quenching processes took place and may account for most of the changes observed in ϕ_{F_o} and ϕ_{F_m}.

During our experiment, zeaxanthin was the major source of absorption variability (Claustre et al. 2002). It showed strong diel changes, with concentration per cell increasing during the whole light period and decreasing during the night. Despite the fact that zeaxanthin induced large variations in the specific absorption coefficient for nonphotosynthetic pigments only (Claustre et al. 2002), these changes are not completely in phase with those of quantum yields of fluorescence (ϕ_{F_x} and $\phi_{F_x}^{PS}$) that decrease only during the morning period (until 1200 h). Moreover, the quantum yields of fluorescence for photosynthetic pigments only (ϕ_{F_x} and $\phi_{F_x}^{PS}$) showed variation amplitudes similar to those of $\phi_{F_o}^{PS}$ and $\phi_{F_m}^{PS}$. On the other hand, zeaxanthin has a turnover time of formation/degradation found to be between 14 and 24 h (Goericke and Welshmeyer 1992; Caillau et al. 1996). These turnover times cannot be considered as similar to the half-life time of recovery from quenching of the quantum yields of fluorescence. Furthermore, even the highest reported cellular content of zeaxanthin in prokaryotic phytoplankton cannot account for significant shading of the cell (see the discussion in Babin et al. 1996). Besides this, it is worth noting that zeaxanthin in the Cyanobacteria is located in the cell wall (Partensky and Garczarek 2003), which prevents it from playing any significant role in changes in the quantum yields of fluorescence. Even if the localization of zeaxanthin remains unclear for *Prochlorococcus* cells, the case of Cyanobacteria should be taken into account. Consequently, zeaxanthin cannot be considered as a major source of variation in the quantum yields of fluorescence.

The almost complete recovery of F_v/F_m at dusk suggests that long-lifetime photoinhibition was unlikely to take place in the PSII reaction center. The strong positive correlation between the rate of transcription of the gene coding for D1 protein (*psbA*) and growth irradiance ($r^2 = 0.81$, $n = 17$) suggests a quasi-instantaneous response of the D1 turnover to increasing photon fluxes, even at nonsaturating levels (Schaefer and Golden 1989). The rapid turnover of D1 molecules allows efficient repair of the PSII reaction center at high light. This phenomenon has been proposed to be a photoprotective mechanism in cyanobacteria (Golden 1995). Such a mechanism may also contribute to the relative insensitivity of this surface strain of *Prochlorococcus* to photoinhibition of PSII reaction center.

Photosynthetic parameters—It is very likely that the initial decrease in ϕ_{Cmax} right after light onset (Fig. 3B) is partly related to large quenching in ϕ_{F_o} and ϕ_{F_m} as well as to the small decrease in F_v/F_m (Fig. 2B) and can therefore be explained by the processes described above. During this initial decrease in ϕ_{Cmax} (0600–1000 h), P_{max}^B increases (Fig. 4B). This last part of the increase in P_{max}^B seems to be triggered by light, as suggested by the step-like pattern observed around 0600 h (Fig. 4B). It could therefore result from the light-dependent activation of Rubisco. This mechanism has been described for phytoplankton by MacIntyre et al. (1997). These opposite changes in ϕ_{Cmax} (and α^B, Fig. 4A) and P_{max}^B are responsible for the increase in E_k observed between 0600 and 1200 h (Fig. 4B).

Between 1000 and 1200 h, both ϕ_{Cmax} (and α^B) and P_{max}^B decrease sharply while E_k varies only slightly. Such covariations in ϕ_{Cmax} (and α^B) and P_{max}^B have often been observed at the daily time scale (Harding et al. 1981*b*; Rivkin and Putt 1988). This covariability could result from the transient occurrence of alternative sinks (i.e., other than reduction of carbon compounds) for the use of reductants produced by photosynthesis (Behrenfeld et al. 2004). In Cyanobacteria, as opposed to many algae and plants, large capacity for reduction of O_2 through Melher reaction and possibly chlororespiration have been reported (Badger et al. 2000). In *Prochlorococcus,* which, like typical phycobilisome-containing cyanobacteria, lacks significant short-lifetime nonphotochemical quenching, similar capacity may exist and serve a role in energy dissipation and recycling. Significant O_2 reduction through photorespiration may also occur. In this context, it is worth noting that many genes encoding proteins (and protein complexes) involved in carbon-concentrating mechanisms found in cyanobacteria such as carbonic anhydrase and specific nicotinamide adenine dinucleotide (NADH) dehydrogenase proteins have not been found in the genome of *Prochlorococcus* (Hess et al. 2001). This observation supports the possible occurrence of photorespiration in *Prochlorococcus.*

After 1200 h and until the night, the decrease in E_k results from a decrease in P_{max}^B as ϕ_{Cmax} (and α^B) are nearly constant during that period (Figs. 3B and 4A) (lag-time correlation between E_k and P_{max}^B between 1200 and 0000 h, Δt = no lag, $r^2 = 0.64$, $n = 20$, other lag times lead to less- or nonsignificant relationships). This decrease in P_{max}^B is accompanied by a decrease in the transcription level of the gene coding for Rubisco (*rbcL*) (Fig. 5). The apparent relationship between *rbcL* mRNA levels and P_{max}^B values, which was previously observed (Pichard et al. 1996), has to be interpreted with some care, as no direct estimation of the Rubisco protein activity was done during the experiment. However, a relationship between P_{max}^B and cell concentration in Rubisco has been evidenced in several phytoplankton species (Orellana and Perry 1992), and it is reasonable to assume that it is true for *Prochlorococcus* as well. Light-dependent deactivation of Rubisco may, however, be responsible as well for the late decrease in P_{max}^B as PAR decreases and in the dark (MacIntyre et al. 1997).

Globally, E_k is generally considered as a good indicator of photoacclimation (Henley 1993). During our experiment, the cyclic variations of E_k over a factor of two and nearly

in phase with the light cycle clearly indicate that *Prochlorococcus* did photoacclimate to diel changes in PAR (Fig. 4B).

A possible effect of cell division on the photosynthetic parameters—During the afternoon and the following 12-h dark period, we observed a slow recovery in ϕ_{F_o} and ϕ_{F_m} (Fig. 2A) as well as in ϕ'_{F_o} and ϕ'_{F_o} (data not shown). The full recovery up to the maximum values only occurred at the end of the dark period. The high K_r (0.283 $\pm$0.052 h^{-1}) value determined at time of maximum PAR is incompatible with such a slow recovery in the cultures. To illustrate this point, we used a model that describes the dynamic changes in the quenching and recovery processes (modified from Neale 1987),

$$\frac{d\phi_F}{dt} = -K_q\tau\sigma_{PS2}\mathrm{PAR}\phi_F + K_r(\phi_{F_i} - \phi_F) \qquad (8)$$

where ϕ_F accounts for either minimum or maximum fluorescence, ϕ_{F_i} is the initial value of the quantum yield, K_q (h^{-1}) is the rate constant for quenching of fluorescence and τ (h) is a turnover time for PS2 photochemistry under continuous light. We first determined K_r as described in the Methods section, using the data from fluorescence yields (note that, in the dark, Eq. 8 becomes a first-order kinetics expression). Using this K_r value, measured σ_{PS2} and PAR, we then estimated the product $K_q\tau$ by fitting Eq. 8 to the ϕ_F data obtained between 0600 and 1000 h. We assumed that, during this period, the first term on the right-hand side of Eq. 8 accounted for most of the ϕ_F variations. This assumption is justified by the fact that the first term on the right-hand side of Eq. 8 must be much higher than the second one to explain the steep decrease observed in ϕ_F during that period. Using ϕ_{F_o}, we obtained, on average, $K_q\tau = 0.56 \pm 0.06$, with reproducible results from one day to another. Finally, we ran Eq. 8 numerically by a step-by-step method using the estimated $K_q\tau$ and K_r values and the measured σ_{PS2} and PAR ones. Our calculations were conducted separately for each day, starting at 0600 h. Therefore, the ϕ_F value obtained at 0600 h was used as ϕ_{F_i}. Note that the 0600-h value increased from one day to the next over the 3 d of sampling by about 20%. To take this slight change into account, we applied a linear interpolation between 0600 h values and thereby obtained an adjusted ϕ_{F_i} for each time step of the calculation.

In Fig. 7, we compare observed and modeled results. For ϕ_{F_o} as well as for ϕ_{F_m}, the modeled values are in agreement with the observed ones during the light period. As soon as the light is switched off, however, the increase in the modeled values is much faster than for the observed ones. This strongly suggests that nonphotochemical quenching alone cannot explain the slow recovery in ϕ_{F_o} and ϕ_{F_m} as well as in ϕ_{Cmax}. When looking closer at the trends in ϕ_{F_o} and ϕ_{F_m} during the recovery phase (Fig. 7), one can notice three distinct periods. In the first one, the quantum yield of fluorescence starts to increase rapidly from 1200 to 2000 h, possibly because of recovery from nonphotochemical quenching, as suggested by the agreement between the modeled and observed values. In the second part, around 2000 h, when the cell division is close to peaking, the variation

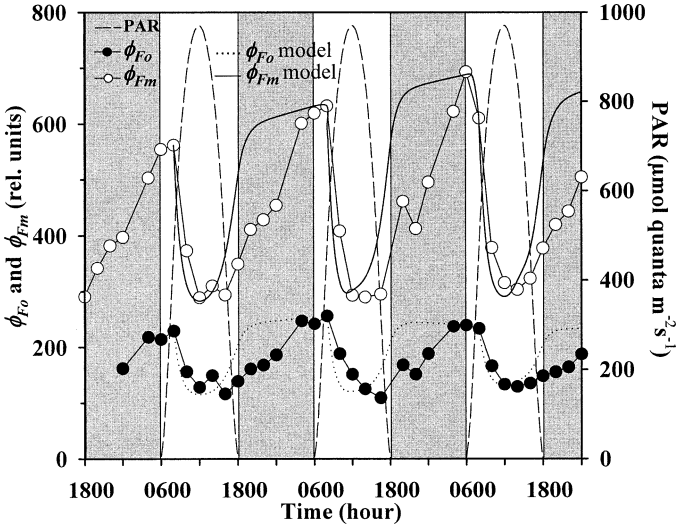

Fig. 7. Diel changes in the PAR (μmol quanta m^{-2} s^{-1}) and in the minimum ϕ_{F_o} and maximum ϕ_{F_m} quantum yield of in vivo chlorophyll *a* fluorescence (relative units), either measured data (circles) or recalculated with the Neale model (lines).

in ϕ_{F_o} and ϕ_{F_m} slows down or even reverses its sign until 0000 h. Finally, in the third part, the increase in the quantum yields of fluorescence is fast again. It starts at 0000 h after the cell division (Fig. 7) and lasts until 0800 h in the morning (see also Holtzendorff et al. 2001). The coincidence between cell division and the slow down in ϕ_{F_o} and ϕ_{F_m} recovery suggests that the cell division cycle may partly govern ϕ_{F_o} and ϕ_{F_m} diel variations, especially at night.

In order to better identify the different processes of the cell cycle that could be involved, we examined the transcription patterns of genes encoding major proteins of the photosynthetic apparatus. The transcription pattern of the *pcbA* gene (encoding the protein part of the light harvesting system of PSII, i.e., the antenna) showed a bimodal rhythm, with a first minimum at the beginning of the light period (0800 h), likely due to light increase (Garczarek et al. 2001). A second minimum was observed during the first part of the night (around 2000 h) coincident with the peak in cell division (Garczarek et al. 2001). We hypothesize that synthesis of PSII antenna (like that of other photosynthetic proteins such as D1 and Rubisco) was inhibited by cell division, which in turn slowed down the recovery of ϕ_{F_o}, ϕ_{F_m}, and ϕ_{Cmax}. After cell division, the increase in ϕ_{F_o}, ϕ_{F_m}, and ϕ_{Cmax} to their highest values (Figs. 2A and 3B) was coincident with the peaks in transcription of the *pcbA* gene (Garczarek et al. 2001).

Effect of diel variations in photosynthetic parameters on carbon fixation—Cumulated amount of carbon fixed per unit div-Chl *a* [Θ^B; mg C (mg div-Chl *a*)$^{-1}$] in cyclostat 1 can be calculated over the course of the day from

$$\Theta^B(t) = \int_0^t P^B(t)\,dt \qquad (9)$$

where $P^B(t)$ is obtained from Eq. 4 without considering P^B_o, and t is the time elapsed in hours since 0600 h. To apply

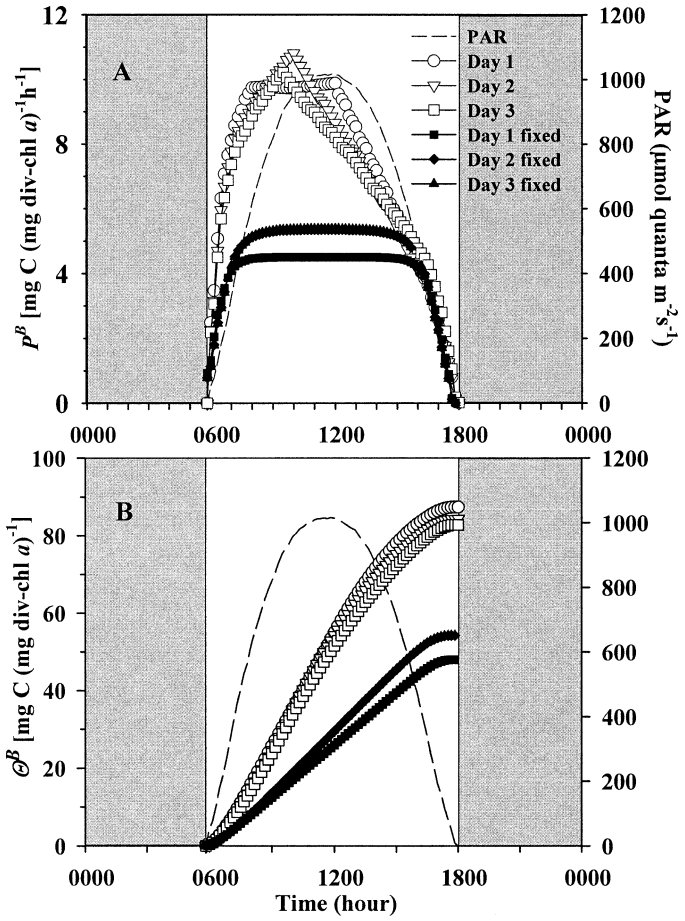

Fig. 8. Carbon accumulation in cyclostat #1 calculated over each light period of the 3-d experiment. (A) P^B instantaneous carbon fixation rate [mg C (mg div-Chl *a*)$^{-1}$ h^{-1}]. (B) Θ^B cumulated fixed carbon values over one light period [mg C [mg div-Chl *a*]$^{-1}$]. The data were interpolated every 10 min with values of P^B_{max} and α^B either fixed (values considered are those of 1400 h, filled symbols) or variable during the day (open symbols).

Eq. 9 to our measurements of light and photosynthetic parameters, α^B has to be modified as in Babin et al. (1996) to account for the difference between the irradiance spectra in the cyclostat and in the incubator, by considering the ratio between $\bar{a}^*$ determined for the cyclostat and that determined for the incubator (Eq. 7). Figure 8 shows calculated values of P_{max} and Θ^B as a function of time for cyclostat 1 and for the 3 d of the experiment (empty symbols). Linear interpolation of measured P^B_{max} and α^B allowed calculations at 10-min intervals.

As a result of diel variations in α^B and P^B_{max}, the P^B versus time relationship is skewed to the left and maximum P^B systematically occurs between 0800 and 1100 h. This pattern differs much from what would be observed with constant α^B and P^B_{max} values (Fig. 8A, dark symbols, with α^B and P^B_{max} values observed at 1400 h as an example). If the diel cycle is taken into account, half of the maximum Θ^B is reached around 1040 h, and two thirds of daily carbon fixation occurs before 1200 h (Fig. 8B). An afternoon depression in carbon fixation has been reported in several studies (Schanz and Dubinsky 1988, and references therein). Our results suggest that this depression is due to the decrease in α^B and P^B_{max} in the afternoon, while in the morning, carbon fixation is achieved at a maximum rate before the photosynthetic apparatus is affected by high irradiance and Rubisco gets deactivated in the afternoon by decrease in light intensity.

The diel variations of the photosynthetic parameters of phytoplankton are often characterized by maxima in α^B and P^B_{max} during the day when midday irradiance is low to moderate and during the night when midday irradiance is high (see Introduction). In this study, where *Prochlorococcus* cells were exposed to high midday irradiance, both α^B and P^B_{max} were maximal at the beginning of the light period, strongly decreased at midday, and remained low until the middle of the dark period. Our results suggest that the initial decrease in α^B and P^B_{max} results from exposure to high irradiance and that the slow recovery by night is related to the cell division cycle. We believe that, under low to moderate irradiance, only the cell cycle drives the diel variations in α^B and P^B_{max}, which leads to lowest values by night, as it has often been observed in natural phytoplankton. To verify this hypothesis, similar experiments will have to be conducted with different midday irradiances. Transfer of the culture to continuous light may also be considered, although synchronization of cell division is, at least for *Prochlorococcus,* rapidly lost under continuous light (Jacquet et al. 2001).

Despite the abundant literature on diel variations of photosynthetic parameters of phytoplankton, there is still not much known about the mechanisms underlying these variations. Only few studies have actually attempted to dissect the phenomenon by analyzing the different structural components and functional properties of the photosynthetic apparatus under controlled conditions. This is what we started to achieve in this study. Still, our results are much descriptive, but they did allow us to clarify to some extent the contribution of nonphotochemical quenching (or photoacclimation in general) and to emphasize the potential role of cell-cycle processes. We believe that this study will open the way to more mechanistic approaches of the problem.

Models that describe and predict phytoplankton growth based on photoacclimation and mass balance have been developed for continuous light conditions and do not account for diel variations in the photosynthetic parameters and other critical cellular processes (Geider et al. 1998). Our study illustrates the constraint imposed by the light cycle and the complexity of the mechanism responsible for these diel variations. How to represent photoacclimation under a natural light cycle is unclear. Also, within a day, balanced growth is never actually achieved because the light and cell cycles impose sequential cellular activities during the course of the day. One of the major challenges in phytoplankton modeling is to consider the natural light cycle and the diel changes it induces in the photosynthetic properties and other critical cellular processes.

References

AXMANN, I. M., H. HERZEL, W. R. HESS, AND J. VOGEL. 2003. Experimental and computational analysis of transcriptional

start sites in the cyanobacterium *Prochlorococcus* MED4. Nucleic Acids Res. **31:** 2890–2899.

BABIN, M. A. MOREL, H. CLAUSTRE, A. BRICAUD, Z. S. KOLBER, AND P. G. FALKOWSKI. 1996. Nitrogen- and irradiance-dependent variations of the maximum quantum yield of carbon fixation in eutrophic, mesotrophic and oligotrophic marine systems. Deep Sea Res. I **43:** 1241–1272.

———, J. C. THERRIAULT, L. LEGENDRE, B. NIEKE, R. REUTER, AND A. CONDAL. 1995. Relationship between the maximum quantum yield of carbon fixation and the minimum quantum yield of chlorophyll *a* in vivo fluorescence in the Gulf of St Lawrence. Limnol. Oceanogr. **40:** 956–968.

BADGER, M. R., S. VONCAEMMERER, S. RUUSKA, AND H. NAKANO. 2000. Electron flow to oxygen in higher plants and algae: rates and control of direct photoreduction (Melher reaction) and Rubisco oxygenase. Philos. Trans. Royal Soc. London, Biol. Sci. **355:** 1433–1446.

BEHRENFELD, M. J., O. PRASIL, M. BABIN, AND F. BRUYANT. 2004. In search of a physiological basis for covariations in light-limited and light-saturated photosynthesis. J. Phycol. **40:** 4–25.

———, ———, Z. S. KOLBER, M. BABIN, AND P. G. FALKOWSKI. 1998. Compensatory changes in photosystem II electron turnover rates protect photosynthesis from photoinhibition. Photosynthesis Res. **58:** 259–268.

BIDIGARE, R. R., M. E. ONDRUSEK, J. H. MORROW, AND D. A. KIEFER. 1990. In vivo absorption properties of algal pigments. Ocean Optics 10, SPIE **1302:** 290–302.

BRUYANT, F., AND OTHERS. 2001. An axenic cyclostat of *Prochlorococcus* strain PCC9511 with a simulator of natural light regimes. J. Appl. Phycol. **13:** 135–142.

CAILLAU, C., H. CLAUSTRE, F. VIDUSSI, D. MARIE, AND D. VAULOT. 1996. Carbon biomass, and gross growth rate as estimated from ^{14}C pigment labelling, during photoacclimation in *Prochlorococcus* CCMP 1378. Mar. Ecol. Prog. Ser. **145:** 209–221.

CAMPBELL, D., V. HURRY, A. K. CLARKE, P. GUSTAFSSON, AND G. ÖQUIST. 1998. Chlorophyll fluorescence analyses of cyanobacterial photosynthesis and acclimation. Microbiol. Mol. Biol. Rev. **62:** 667–683.

CARPENTER, E. J., AND J. CHANG. 1988. Species specific phytoplankton growth rates via diel DNA synthesis cycles. I. Concept and methods. Mar. Ecol. Prog. Ser. **43:** 105–111.

CLAUSTRE, H., A. BRICAUD, M. BABIN, F. BRUYANT, L. GUILLOU, AND F. PARTENSKY. 2002. Diel variations in *Prochlorococcus* optical properties. Limnol. Oceanogr. **47:** 1637–1647.

DANDONNEAU, Y., AND J. NEVEUX. 1997. Diel variations of in vivo fluorescence in the eastern equatorial Pacific: An unvarying pattern. Deep Sea Res. II **44:** 1869–1880.

DUBINSKY, Z. 1980. Light utilization efficiency in natural phytoplankton communities, p. 83–97. *In* P. G. Falkowski [ed.], Primary productivity in the sea. Plenum.

FALKOWSKI, P. G., AND J. A. RAVEN. 1997. Aquatic Photosynthesis. Blackwell.

GARCZAREK, L., W. R. HESS, J. HOLTZENDORFF, G. W. M. VAN DER STAAY, AND F. PARTENSKY. 2000. Multiplication of antenna genes as a major adaptation to low light in a marine prokaryote. Proc. Natl. Acad. Sci. USA **97:** 4098–4101.

———, F. PARTENSKY, H. IRLBACHER, J. HOLTZENDORFF, M. BABIN, I. MARY, J. C. THOMAS, AND W. R. HESS. 2001. Differential expression of antenna and core genes in *Prochlorococcus* PCC 9511 grown under a light-dark cycle. Env. Microbiol. **3:** 168–175.

GEIDER, R. J., H. L. MACINTYRE, AND T. M. KANA. 1998. A dynamic regulatory model of phytoplanktonic acclimation to light, nutrients, and temperature. Limnol. Oceanogr. **43:** 679–694.

GOERICKE, R., AND N. A. WELSCHMEYER. 1992. Pigment turnover in the marine diatom *Thalassiosira weissflogii*. II. The $^{14}CO_2$-labelling kinetics of carotenoids. J. Phycol. **28:** 507–517.

GOLDEN, S. S. 1995. Light-responsive gene expression in Cyanobacteria. J. Bacteriol. **177:** 1651–1654.

———, M. ISHIURA, C. HIRSCHIE JOHNSON, AND T. KONDO. 1997. Cyanobacterial circadian rhythms. Annu. Rev. Plant Physiol. Plant Mol. Biol. **48:** 327–354.

HARDING, L. W. J., B. W. MEESON, B. B. PRÉZELIN, AND B. M. SWEENEY. 1981*a.* Diel periodicity of photosynthesis in marine phytoplankton. Mar. Biol. **61:** 95–105.

———, B. B. PRÉZELIN, B. M. SWEENEY, AND J. L. COX. 1981*b.* Diel oscillations in the photosynthesis-irradiance relationship of a planktonic marine diatom. J. Phycol. **17:** 389–394.

HENLEY, W. J. 1993. Measurement and interpretation of photosynthetic light-response curves in algae in the context of photoinhibition and diel changes. J. Phycol. **29:** 729–739.

HESS, W. R., C. FINGERHUT, AND A. SCHON. 1998. RNAse P RNA from *Prochlorococcus marinus*: Contribution of substrate domains to recognition by a cyanobacterial ribozyme. FEBS Lett. **431:** 138–142.

———, G. ROCAP, C. S. TING, F. LARIMER, S. STILWAGEN, J. LAMERDIN, AND S. W. CHISHOLM. 2001. The photosynthetic apparatus of *Prochlorococcus*: Insight through comparative genomics. Photosynthesis Res. **70:** 53–71.

———, A. WEIHE, S. LOISEAUX-DE-GOER, F. PARTENSKY, AND D. VAULOT. 1995. Characterization of the single *psbA* gene of *Prochlorococcus marinus* CCMP 1375 (Prochlorophyta). Plant Mol. Biol. **27:** 1189–1196.

HOLTZENDORFF, J., AND OTHERS. 2001. Diel exression of the cell cycle-related genes in synchronized cultures of *Prochlorococcus* sp. strain PCC 9511. J. Bacteriol. **183:** 915–920

———, D. Marie, A. F. Post, F. Partensky, A. Rivlin, and W. R. Hess. 2002. Synchronized expression of *ftsZ* in natural *Prochlorococcus* populations of the Red Sea. Env. Microbiol. **4:** 644–653.

JACQUET, S., F. PARTENSKY, D. MARIE, R. CASOTTI, AND C. VAULOT. 2001. Cell cycle regulation by light in *Prochlorococcus* strains. Appl. Environ. Microbiol. **67:** 782–790.

JASSBY, A. D., AND T. PLATT. 1976. Mathematical formulation of the relationship between photosynthesis and light for phytoplankton. Limnol. Oceanogr. **21:** 540–547.

KIEFER, D. A. 1973. Chlorophyll a fluorescence in marine centric diatoms: Responses of chloroplasts to light and nutrient stress. Mar. Biol. **23:** 39–46.

KOLBER, Z. S., O. PRASIL, AND P. G. FALKOWSKI. 1998. Measurements of variable fluorescence using FRR technique: Defining methodology and experimental protocols. Biochim. Biophys. Acta **1367:** 88–106.

KRAUSE, G. H., AND E. WEISS. 1991. Chlorophyll fluorescence and photosynthesis: The basics. Annu. Rev. Plant Physiol. Plant Mol. Biol. **42:** 313–349.

LEWIS, M. R., AND J. C. SMITH. 1983. A small volume, short-incubation-time method for measurements of photosynthesis as a function of incident irradiance. Mar. Ecol. Prog. Ser. **13:** 99–102.

MACINTYRE, H. L., T. D. SHARKEY, AND R. J. GEIDER. 1997. Activation and deactivation of ribulose-1,5-bisphosphate carboxylase/oxygenase (Rubisco) in three marine microalgae. Photosynthesis Res. **51:** 93–106.

MARIE, D., F. PARTENSKY, D. VAULOT, AND C. BRUSSAARD. 1999. Enumeration of phytoplankton, bacteria, and viruses in marine samples, p. 11.11.1–11.11.15. *In* Current protocols in cytometry. Wiley.

———, N. SIMON, L. GUILLOU, F. PARTENSKY, AND D. VAULOT. 2000. DNA/RNA analysis of phytoplankton by flow cytometry, p. 11.12.1–11.12.14. *In* Current protocols in cytometry. Wiley.

MAUZERALL, D. C. 1972. Light-induced changes in *Chlorella*, and the primary photoreaction for the production of oxygen. Proc. Natl. Acad. Sci. USA **69:** 1358–1362.

NEALE, P. J. 1987. Algal photoinhibition and photosynthesis in the aquatic environment, p. 39–65. *In* D. J. Kyle, C. B. Osmond, and C. J. Arntzen [eds.], Photoinhibition. Elsevier.

ORELLANA, M. V., AND M. J. PERRY. 1992. An immunoprobe to measure Rubisco concentrations and maximal photosynthetic rates of individual phytoplankton cells. Limnol. Oceanogr. **37:** 478–490.

PARKHILL, J.-P., G. MAILLET, AND J. J. CULLEN. 2001. Fluorescence-based maximal quantum yield for photosystem II as a diagnostic of nutrient stress. J. Phycol. **37:** 517–529.

PARSONS, T. R., Y. MAITA, AND C. M. LALLI. 1984. Photosynthesis as measured by the uptake of radioactive carbon, p. 115–120. *In* R. Maxwell [eds.], A manual of chemical and biological methods for seawater analyses. Pergamon.

PARTENSKY, F., J. BLANCHOT, AND D. VAULOT. 1999*a*. Differential distribution and ecology of *Prochlorococcus* and *Synechococcus* in oceanic waters: A review, p. 431–449. *In* L. Charpy and A. W. D. Larkum [eds.], Marine Cyanobacteria. Institute of Oceanography Monaco.

———, AND L. GARZAREK. 2003. The photosynthetic apparatus of chlorophyll *b*- and *d*-containing oxyphotobacteria, p. 29–62. *In* A. W. D. Larkum, S. E. Douglas, and J. A Raven [eds.], Photosynthesis in algae. V. 14. Kluwer.

———, W. R. HESS, AND D. VAULOT. 1999*b*. *Prochlorococcus*, a marine photosynthetic prokaryote of global significance. Microbiol. Mol. Biol. Rev. **63:** 106–127.

PICHARD, S. L., L. CAMPBELL, J. B. KANG, F. R. TABITA, AND J. H. PAUL. 1996. Regulation of ribulose biphosphate carboxylase gene expression in natural phytoplankton communities. I. Diel rhythms. Mar. Ecol. Prog. Ser. **139:** 257–265.

PRÉZELIN, B. B., AND H. A. MATLICK. 1980. Time-course of photoadaptation in the photosynthesis-irradiance relationship of a dinoflagellate exhibiting photosynthetic periodicity. Mar. Biol. **58:** 85–96.

PRIESTLEY, M. B. 1994. Probability and mathematical statistics, a series of monographs and textbooks: Spectral analysis and time series. Academic.

PUTT, M., AND B. B. PRÉZELIN. 1988. Diel periodicity of photosynthesis and cell division compared in *Thalassiosira weissflogii* (Bacillariophyceae). J. Phycol. **24:** 315–324.

RIPPKA, R., AND OTHERS. 2000. *Prochlorococcus marinus* Chisholm et al. 1992, subsp. nov. *pastoris*, strain PCC9511, the first axenic chlorophyll a_2/b_2-containing cyanobacterium (Oxyphotobacteria). Int. J. Syst. Evol. Microbiol. **50:** 1833–1847.

RIVKIN, R. B., AND M. PUTT. 1987. Diel periodicity of photosynthesis in polar phytoplankton: Influence on primary production. Science **238:** 1285–1288.

———, AND ———. 1988. Seasonal pattern of diel periodicity in the photosynthesis by polar phytoplankton: Species-specific responses. J. Phycol. **24:** 369–376.

SCHAEFER, M. R., AND S. S., GOLDEN. 1989. Differential expression of members of a cyanobacterial *psbA* gene family in response to light. J. Bact. **171:** 3973–3981.

SCHANZ, F., AND Z. DUBINSKY. 1988. The afternoon depression in primary productivity in a high rate oxidation pond (HROP). J. Plank. Res. **10:** 373–383.

STEGLICH, C., AND OTHERS. 2001. Nitrogen deprivation strongly affects photosystem II but not phycoerythrin level in the chlorophyll *b*-possessing cyanobacterium *Prochlorococcus marinus*. Biochim. Biophys. Acta **1503:** 341–349.

VANDEVELDE, T. L. LEGENDRE, S. DEMERS, AND J. C. THERRIAULT. 1989. Circadian variations on photosynthetic assimilation and estimation of daily phytoplankton production. Mar. Biol. **100:** 525–531.

VAULOT, D., AND D. MARIE. 1999. Diel variability of photosynthetic picoplankton in the equatorial Pacific. J. Geophys. Res. **104:** 3297–3310.

VIDUSSI, F., H. CLAUSTRE, J. BUSTILLOS-GUZMAN, C. CAILLIAU, AND J. C. MARTY. 1996. Determination of chlorophylls and carotenoids of marine phytoplankton: Separation of chlorophyll a from divinyl-chlorophyll *a* and zeaxanthin from lutein. J. Plank. Res. **18:** 2377–2382.

Received: 21 July 2004
Accepted: 7 October 2004
Amended: 4 January 2005